

MULTITEMPORAL RADARSAT-2 POLARIMETRIC SAR DATA FOR URBAN LAND-COVER MAPPING

X. Niu^a, Y. Ban^{a,*}

^a Division of Geoinformatics, Department of Urban Planning and Environment,
Royal Institute of Technology, SE-10044 Stockholm, Sweden- (xin.niu, yifang.ban)@abe.kth.se

KEY WORDS: Land cover, classification, SAR, hierarchical, multitemporal

ABSTRACT:

The objective of this research is to evaluate multi-temporal RADARSAT-2 polarimetric SAR data for urban land-cover classification using a novel classification scheme. Six-date RADARSAT-2 Polarimetric SAR data in both ascending and descending orbits were acquired during June to September 2008 in the rural-urban fringe of the Greater Toronto Area. The major land-cover types are built-up areas, roads, golf courses, forest, water and several types of agricultural crops. In this research, the different urban land-cover types and their corresponding polarimetric behaviors were studied. The polarimetric signatures of the various urban land-cover types were extracted from the RADARSAT-2 SAR images and analyzed using a new hierarchical multitemporal classification method. The results showed that the new classification method yielded high classification accuracy, with overall accuracy of 82.1% and Kappa coefficient 0.80 for the major 11 land-cover classes. The classification scheme can effectively extract the urban structures by mapping urban related classes such as streets and major roads with the higher user's accuracy, which is difficult to achieve using a single-date data.

1. INTRODUCTION

In 2008, the world crossed an invisible but momentous milestone: the point at which more than half the people on the planet living in cities (The World Watch Institute, 2007). Urbanization and the impact of human settlements are two of the main causes of global environmental degradation. Therefore, mapping and monitoring urban landuse/land-cover and their changes in a timely and accurate manner is of critical importance for sustainable urban planning and environment protection (Ban *et al.*, 2010). With the launch of advanced remote sensors in recent years such as RADARSAT-2 SAR and TerraSAR-X, multi-temporal, high-resolution, polarimetric SAR data are becoming routinely available for surveying fast expanding urban areas.

Comparing with the single-polarization SAR data, Polarimetric SAR data provide the description of the land features from the observations of various polarizations. Thus, more information can be explored for classification. In the literature, the studies of the polarimetric SAR data focus on the generation of the efficient descriptors from the scattering coefficients and introducing those descriptors to the conventional classification methods. The Cloude/Pottier decomposition (Cloude and Pottier, 1997) and freeman decomposition (Cloude and Pottier, 1996) are well-known examples.

To improve the classification accuracy, multitemporal data have been used whenever the data are available (e.g., Ban & Howarth, 1999; Goodenough & Chen, 2005; Waske *et al.*, 2006). The advantages of the multitemporal classification could be given in the following aspects. (1) The rarely changed parts in different dates will confirm each other to increase the credibility. (2) The temporal attributes could be exploited for certain classes such as

crops. (3) Data from different orbit, for example ascending and descending, will provide complement views of the observed scenes. Various studies have been conducted using multi-temporal and/or polarimetric SAR data. For examples, Galli *et al.* (2007) investigated a joint segmentation technique on a sequence of multi-temporal single-channel SAR images to improve the classification. Tan *et al.* (2007) assessed SVM classifier for classification of crops using multi-temporal Polarimetric SAR data. Park and Chi (2006) investigated a fuzzy logic fusion of multi-temporal multi-polarization SAR data for landcover classification. Shimabukuro *et al.* (2007) led a case study on the mapping of the deforested area using multi date JERS-1 SAR data with HH polarization. Goodenough & Chen (2005) fused the Polarimetric SAR data sets from winter and summer to map the different forest types. Waske *et al.* (2006) used the decision tree to map urban and rural using the multi-date data. Chen *et al.* (2007) explored the feasibility of residential and rural area classification using multi-temporal SAR images using knowledge-based approach.

Few studies, however, used high-resolution polarimetric SAR data for urban analysis due to data availability. And to the best of our knowledge, there is no research on the classification of the high-resolution RADARSAT-2 polarimetric SAR data in urban areas.

Furthermore, using the high-resolution SAR data also poses new challenges on urban land-cover classification due to the complexity of the urban environment. Thereby, it is necessary to exploit the contextual and spatial information as well as knowledge-based approach to improve classification results (Ban and Hu, 2007; Ban *et al.*, 2010).

Thus, in this paper, we propose a new rule-based hierarchical classification method, using multitemporal Polarimetric SAR data to map urban land-cover and extract the fine urban

* Corresponding author

structures. The specific objectives are: 1. to evaluate the capacity of the RADARSAT-2 fine-beam polarimetric SAR for the urban mapping; and 2. to investigate the effectiveness of the proposed multitemporal classification schemes.

2. STUDY AREA AND DATA DESCRIPTION

The study area is located in the north and northwest of the Greater Toronto Area (GTA), Ontario, Canada, where rapid urban expansion is underway. The major land use/land-cover classes in the rural-urban fringe area are high-density area, low-density area, wide roads and airports, path, parks, golf courses, forests, water and several types of crops. Those classes were chosen to characterize the complex area.

The data used for this research consist of six-date RADARSAT-2 fine-beam polarimetric SAR (PolSAR) data, which contain the HH, HV, VH and VV polarizations. The centre frequency at this beam mode is 5.4GHz, i.e., C-band and the spatial resolution is 8 meters. The detailed descriptions of these images are given in Table 1.

Data	Orbit	Incident angle range (degree)
Jun. 11 2008	Ascending	40.179~ 41.594
Jun. 19 2008	Descending	40.215~ 41.619
Jul. 05 2008	Ascending	40.182~ 41.597
Aug. 06 2008	Descending	40.197~ 41.612
Aug. 22 2008	Ascending	40.174~ 41.590
Sep. 15 2008	Ascending	40.173~ 41.588

Table 1. RADARSAT-2 Fine-Beam SAR Imagery

The six-date SAR data are acquired during June to September in 2008, when most of the crops experienced the seasons from flourish to harvest. In contrast, the urban area kept stable in such a short term. Two data groups are naturally formed according to their orbit mode. Thus, the June 11, July 05, August 22, September 15 images make up the ascending group while the June 19, August 06 comprise the descending group.

The different orbit modes introduce different views of the observed objects, which can be used to complement each other. However the angles also pose a challenge to image registration due to the different radar look directions.

In spite of that, all the data are collected in the similar incident angles. Hence the multi temporal data within each group could match each other well, which will benefit the multitemporal classification.

3. METHOD

The proposed hierarchical object-based rule-based classification is illustrated in Figure 2. First, the whole scene was segmented at multi scales using the Pauli parameters derived from the filtered raw Polarimetric SAR data. Secondly, land-cover/land use classes were extracted into different feature layers. Finally we combine those layers in hierarchy according to their

credibility levels. The multitemporal feature extraction schemes lies in two aspects: 1. The layer of urban and rural is the classification result on the stacked multi-date data. 2. Any other layer is the fusion result of that specific class from multiple single-date classifications.

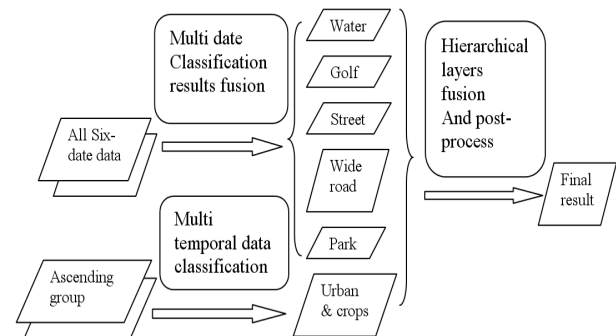


Figure 2. Multitemporal classification scheme

3.1 Orthorectification and Registration

All the six-date RADARSAT-2 fine-beam polarimetric SAR data are orthorectified by the DEM with resolution of 30m. Then all the data are registered to the National Topographic Database (NTDB) vector data. The images could overlay each other well that all the streets are perfectly matched, especially for data in the same orbit mode, i.e., ascending or descending. That excellent overlapping is the base for our multitemporal classification scheme.

3.2 Preprocessing and Pauli decomposition

First, we extract the hermitian coherency matrix $\langle T \rangle$ for all the raw polarimetric SAR data. The coherency matrix was then filtered by Lee refined filter (Lee, 1981). The number of looks and the window size are set as 2 and 7 respectively. The Pauli parameters are directly obtained as the diagonal elements of the coherency matrix $\langle T \rangle$.

The Pauli parameters (Cloude and Pottier, 1996): $|\text{HH}+\text{VV}|$, $|\text{HH}-\text{VV}|$, $|\text{HV}|$ are the measurements of the relative powers of the three physical models: odd-bounce, dihedral oriented at 0 degrees and volume scattering. The real examples for the above models are rough surface, urban building and vegetation respectively. Since the total power of the targets is equal to that of the backscattering matrix. It is often used for illustration.

Although we do not use all the other elements in the coherency matrix $\langle T \rangle$, i.e., the real and image parts of $(\text{HH}+\text{VV})(\text{HH}-\text{VV})^*$, $(\text{HH}+\text{VV})\text{HV}^*$ and $(\text{HH}-\text{VV})\text{HV}^*$ which together represent all the polarization information, the Pauli parameters could present the most contrast between the land-cover/land use classes. In this experiment, the logarithm (base 10) of the Pauli parameters is used as the spectral channels for classification.

3.3 Multi-Scale Segmentation with eCognition

In the experiments, the multiresolution segmentation algorithm in eCognition is selected as the segmentation method. This segmentation technique aims to locally maximize the homogeneity within the objects. This process, which starts from the pixel level, iteratively aggregates the neighboring candidate segments until they reach the given scale. The homogeneity criterion makes a trade-off between the spectral and spatial domain. In spectral domain, the homogeneity is decided by the

standard deviation, while in the shape domain, there is a balance between the compactness and smoothness. (Baatz *et al.*, 2004).

In this research, multi-scale segmentation hierarchy is constructed for each single date data. This hierarchy has three segmentation levels whose scales are 50, 100 and 200. The higher level is the merge result of the lower level. The shape and compact parameters for segmentation are set as 0.4 and 0.5 for the scale 50, 0.5 and 0.5 for the scale 100 and 200. Those empirical segmentation parameters for all the date data are selected by trials and comparisons.

The reasons for using the hierarchical multi-scale segmentation layers are: 1. The land-cover/land use type needs appropriate shape size to be represented. For instance, the water pond, golf course area are directly extracted from the smaller scale/higher level layer, while the streets are from the larger scale/lower level layer. 2. The relationship between the super or sub segmentation layers offers spatial information of the object's surroundings. For example, the mapping of the park benefits from the information from the classification of higher level/smaller scale segmentation layer.

3.4 Rule-based Class Layer Extraction and Multitemporal Fusion

As mentioned, the class layer of water, street, wide road, golf or park is the fusion of that specific class from multiple single-date classification results. However, the urban and rural areas are classified on the stacked multi-date data. The golf course class is extracted from the segmentation level with scale of 200 and wide road and water from the level of scale 100 while the rest are from the level of scale 50.

The advantages of the hierarchical layers extraction could be in two folds: 1. We can focus on some specific land-cover classes to specifically improve their classification accuracy. 2. Different layer fusion schemes can be employed for different purposes (e.g., to achieve high user's accuracy or producer's accuracy).

The rules involved in the classification consist of criterions considering the objects' data value and shape. On one hand, for the classes such as water, forest, crops and urban which are distinguished by the data value, the standard nearest neighbor classifier is applied to obtain the initial classification results based on the samples. Since the segmentation results are various for different date data, the samples are not exactly the same for all the date data, but they all collected from the same area. On the other hand, the road and street are extracted by the shape characters and the relationships with the neighboring classes. Following are the descriptions of such rules and fusion schemes for each class.

3.4.1 Water: The water class is extracted by standard nearest neighbor classifier with the mean values and the standard deviation on scale 100. On this level, most of the ponds are segmented as an entire part. Thus, the other small low scattering objects like the shadow will be excluded from this level and not mistaken as water.

The water area extracted from the single date has higher accuracy. However, some turbid ponds has the scattered values behaved differently in one looking direction and another. For instance, in figure 3, the pond from June 11 (ascending) has higher scattered values while in June 19 (descending) it has

normally low values. Therefore, first we make the intersection of the water layers within each ascending or descending group. Then, the two group intersection layers are combined as the final water layer.

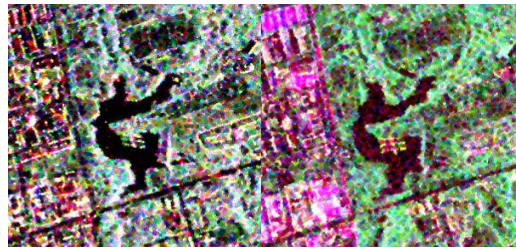


Figure 3. Comparison of the Pauli image of the water pond . From left to right are ponds from June 19 (descending) and June 11(ascending)

3.4.2 Golf Course: The golf course is a complex area consists of grass, pond, bare field and some houses. However, at the higher segmentation scale, those adjacent ingredients can form a distinct part from the surrounding. It can be found from figure 4 that at scale 200, the golf area is well segmented and distinct from the other part. Thus the golf is extracted by standard nearest neighbor classifier with the mean values and the standard deviation on scale 200.

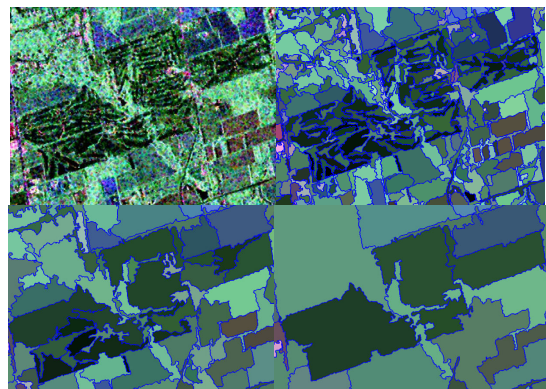


Figure 4. Comparison of segmentation results of different scale size of the golf area. From top left to bottom right are the golf Pauli image from June 19 and its segmentation result of scale 50,100 and 200.

Since the segmentation result is not always perfectly matched the golf area, thus the fusion layers formed by stacking the golf class from all the dates. If in some area the overlap time exceeds certain threshold, this area will be labeled as golf course.

3.4.3 Street: The streets are distinguished on scale 50 by its shape characters and the relationship with the urban area. The street segment should be the narrow winding object which has the higher roundness (defined by the difference of the radius of the smallest enclosing ellipse and the largest enclosed ellipse) and lower rectangular fit (defined as the fitness to the rectangle which has the same area). The width of the skeleton of the street should be smaller. And it should border on more urban objects.

The fusion scheme of the street layer is similar to the golf layer.

3.4.4 Wide road: Similar to the street, the wide road is mainly extracted by the shape characters. Comparing with the street, the wide road has wider width, and less curves. Thus, the longer wider segment will be marked as wide road. Thereby, the rules would consider the ratio of the length to the width, the width range. Furthermore, the flat road usually has lower scattering. Since the wide roads often run through the urban area, it has higher contrast to the brighter neighbor objects.

Those criteria are combined to map the wide road of each single date on the segmentation level of scale 100. Then the results from multi date fuse like the process of the street layer.

3.4.5 Park: The park is defined as the vegetation or bare field embedded in the urban area. Thus the initial classified crops enclosed by the urban patch will be marked as park. However, the scattered odd man made structures in the rural will lead the mistakes by labeling the adjacent crops as park. Thus, we first map those areas with scattered houses embraced by crops as rural on the higher segmentation level of scale 100 to avoid such error. Then the park will be marked at the lower level of scale 50 based on the relationship both to the super and neighboring objects. The multi date result fusion is the same to road.

3.4.6 Rural and urban: The rural and urban area (including the forest) is simply segmented and mapped on the stacked ascending data group, using the standard nearest neighbor classification with the mean value and standard deviation of the data. We do not choose the descending group to distinguish the urban and rural because of its poor performance to discriminate the low density area from the forest. Since the ascending group has four date data from different seasons, the multi-temporal character of crops can be explored to improve the classification accuracy. Figure 5 gives the illustration of 2 kinds of crops in the time sequence of ascending group.

3.5 Hierarchical Fusion Scheme and Post-processing

All the class layers are one by one input as the thematic maps given the rural and urban layer as the base layer to be fused on. While one class layer are being fused, on the base layer, the objects which were covered by the class feature beyond certain portion will be labeled as that class. It is to avoid the scraps as if we directly superimpose the class layers on the base layer, since our class layers are the fusion from different segmentation results. The labeling process is in the order of layer of park, wide road, street, golf and water. The higher the hierarchical layers, the more accurate they are, and less confused with the others. The credibility of the class layers depends on the class' character and the extracting schemes. For example, the park is often confused with street, wide road, thus, it will be mapped below those two layers. The golf course often contains ponds, thus the water layer is on it.

Post-processing consists of two approaches: 1. On the fused map, we strict certain criteria to mark the potential objects for specific classes as we get the fused map with higher accurate context information than the single date data. For example, some potential streets in the fused map may be found and connected. 2. The map is filtered to remove the tiny isolated objects within another class. For example, the shadows or the trunks in the forest area could be removed.

3.6 Accuracy Assessment

For the accuracy test, the Quick-bird images, NTDB vectors and maps are referred. Test areas which contain more than 2000 pixels for each class are randomly selected. The quality of the classification results is assessed by various parameters such as overall accuracy and Kappa coefficient of agreement (or Kappa). They were analyzed to compare classification results with the reference data in confusion matrices.



Figure 5. The temporal character of crop 2 (top 4 Pauli images) and crop 3 (bottom 4 Pauli images), from left to right are from June 19, July 05, August 22 and September 15. All from ascending groups.

4. RESULT AND DISCUSSION

For 11 urban land-cover classes, the overall classification accuracy of 82.1% and Kappa coefficient 0.80 are achieved using our method. The confusion matrix (Table 6) shows that HD, LD, Forest, Water and Agriculture are classified very well. Water (96.66%) and low density area (88.42%) achieve very good accuracies. Park (72.08%) and golf course (75.4%) have relatively lower accuracies as they are difficult to be discriminated from crops or water ponds due to the similar backscattering. As a result of our strict fusion rules, however, they could achieve higher user accuracies. The wide roads (80.76%) and streets (80.63%) are well classified to illustrate the urban structures. Figure 7 shows the example of the wide road and street layers.

The character of our multitemporal classification scheme can be seen from the table that the classes of man-made categories have higher user accuracies. Because rules for those class layers are carefully defined in our fusion schemes, like park and golf. Although the wide road has relatively lower user's accuracy (79.54%), it is caused by the vague definition between street and itself. That is why wide road had a large omission error to street. But if we uniformly treat those two classes as road, the accuracy will definitely become much higher.

The park class has the most complicated situation. Not all the vegetation within the enclosed in the urban area are parks, and there are some parks on the fringe of the urban as well. That makes the rules for identifying parks difficult. The crops are mainly confused among themselves and with the park class.

Reference data (Percent)												
Class	Water	HD	LD	Crop1	Crop2	Crop3	Road	Street	Golf	Forest	Park	User's Accuracy
Water	96.66	0.00	0.00	0.00	0.00	0.00	0.00	1.56	2.12	0.00	0.00	93.11
HD	0.00	82.44	4.79	0.00	0.00	0.00	0.00	1.17	0.00	4.73	0.00	84.76
LD	0.00	14.42	88.42	0.00	0.00	0.00	1.57	9.24	0.00	0.00	0.00	74.97
Crop1	0.00	0.00	0.00	81.27	10.68	20.92	3.97	0.53	15.12	6.35	20.48	31.14
Crop2	0.00	0.00	0.00	8.94	87.48	0.00	0.00	0.00	0.00	0.00	0.00	95.07
Crop3	2.41	0.00	0.00	0.00	1.84	79.08	2.66	0.57	1.74	1.62	0.00	88.62
Road	0.92	1.64	0.00	0.00	0.00	0.00	80.76	0.76	2.57	0.52	5.16	79.54
Street	0.00	0.13	0.00	0.00	0.00	0.00	10.95	80.63	0.00	0.00	2.28	91.81
Golf	0.00	0.00	0.00	0.00	0.00	0.00	0.00	0.00	75.04	0.00	0.00	100.00
Forest	0.00	0.00	0.58	0.00	0.00	0.00	0.00	0.00	2.10	86.78	0.00	97.33
Park	0.00	1.37	6.21	9.79	0.00	0.00	0.00	0.09	5.53	1.31	72.08	80.33
Producer's Accuracy	96.66	82.44	88.42	81.27	87.48	79.08	80.76	80.63	75.04	86.78	72.08	

Table 6. Confusion Matrix.



Figure 7. The wide road structure (left) and part of the street layer (right)

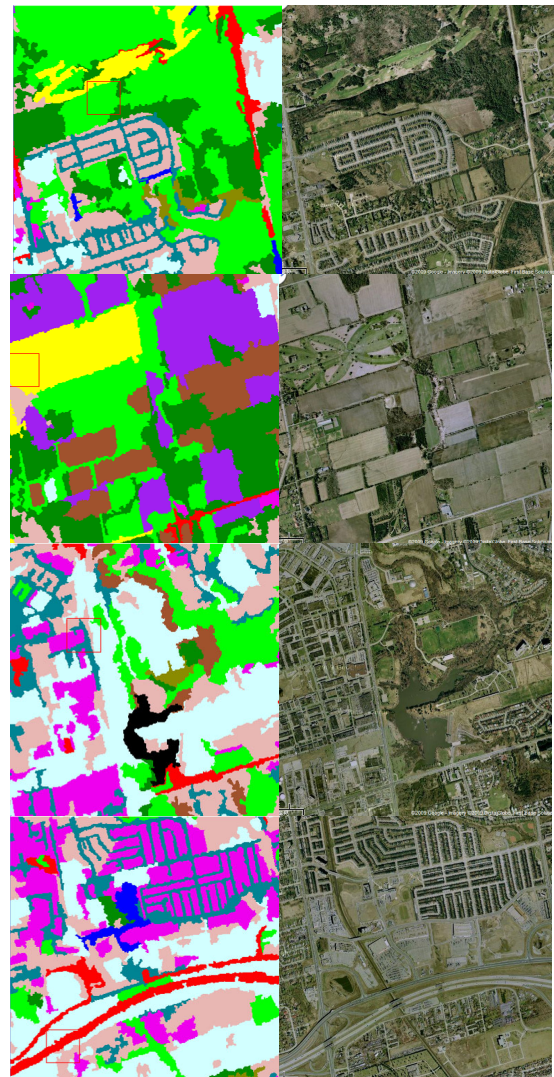
Figure 8 illustrates four examples from our classification result compared with the Quickbird images. It is observed that the classification of built-up areas, wide road, street networks, golf course, and agricultural fields match the features in the Quickbird images very well.

Comparing with the previous multitemporal classification methods such as Chen *et al.* (2007) and Park and Chi (2006), the novelty of our method could be summarized in the following way: 1. Our method combines the hierarchical fusion schemes with the multitemporal conception thus could offer robust and high accuracy for specific classes, while the previous method could only treat all the classes with the same criterions. 2. Comparing the other urban studies such as Waske *et al.* (2006), we could offer more classes to reflect the finer urban structures, while most of the previous studies only focus on mapping the whole urban area. And even there are considerations of the structure mapping, their methods are mostly directed for the wide, major roads extraction, while our scheme propose a efficient way enable to explore the finer structures like streets and parks.

5. CONCLUSIONS

RADARSAT-2 fine-beam polarimetric SAR data were evaluated for land-cover mapping in the rural-urban fringe of the Greater Toronto Area. The multi-temporal hierarchical fusion method applied on the six-date data generates higher classification result, with overall accuracy of 82.1% and Kappa coefficient 0.80 for the major 11 land-cover classes including high-density built-up areas, low-density built-up areas, wide

roads, street, forests, parks, golf courses, water and several types of agricultural lands. The results indicated that the fusion scheme can effectively extract the urban structure by mapping urban related classes such as streets and major roads with the higher user's accuracy, which is difficult to achieve using a single-date data.



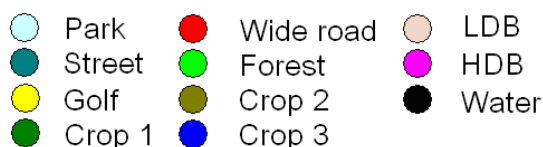


Figure 8. Land-cover classification: selected examples, each comparison consists pair of classification result and the Quickbird reference map.

REFERENCE

- Baatz M., Bentz U., Dehghani S., Heynen M., 2004. eCognition User Guide 4. Definiens Imaging, Muenchen.
- Ban, Y. and P.J. Howarth. 1999. Multitemporal ERS-1 SAR data for crop classification: a sequential-masking approach. *Canadian Journal of Remote Sensing*, Vol. 25, No. 5, pp. 438-447.
- Ban, Y. and H. Hu, 2007. RADARSAT Fine-Beam Data for Land-Cover Mapping and Change Detection in the Rural-Urban Fringe of the Greater Toronto Area. In: *Urban Remote Sensing Joint Event, 2007*, Paris, France, pp.1-7, 11-13.
- Ban, Y., H. Hu and I. Rangel. 2010. Fusion of Quickbird MS and RADARSAT SAR data for urban land-cover mapping: object-based and knowledge-based approach. *International Journal of Remote Sensing*, Volume 31 Issue 6, 1391
- Chen, F.L. Wang, C. Zhang, H., 2007. SAR images classification using case-based reasoning method. In: *IEEE International Geoscience and Remote Sensing Symposium, 2007*, Barcelona, Spain, pp.2048-2051.
- Cloude, S.R. and Pottier, E., 1997. Application of the H/A/alpha polarimetric decomposition theorem for land classification. *Proc. SPIE*, Vol. 3120, pp.132-143.
- Cloude, S.R. and Pottier, E., 1996. A review of target decomposition theorems in radar polarimetry. *IEEE Transactions on Geoscience and Remote Sensing (GRS)*, vol. 34, no. 2, pp. 498–518.
- Galli, L., Passaro, D. and Avolio S., 2007. A Multi-scale Joint Segmentation Technique for Multitemporal and Multisource Remote Sensing Images. *Image and Signal Processing for Remote Sensing, XIII.*, Volume 6748, pp. 674804.
- Goodenough, D.G. and Chen, H., 2005. Multitemporal Evaluation with ASAR of Boreal Forests. In: *IEEE International Geoscience and Remote Sensing Symposium, 2005*, Seoul, South Korea, Vol.3, pp.1662-1665
- Lee, J. S., 1981. Refined filtering of images using local statistics. *Computer Graphics and Image Processing*, Vol. 15, pp. 380-389.
- Park, N.-W. Chi, K.-H., 2006. Land-cover classification using multi-temporal /polarization C-band SAR data. In: *IEEE International Geoscience and Remote Sensing Symposium, 2006*, Denver, USA, pp.188-191
- Shimabukuro, Yosio E., Raimundo Almeida-Filho, Tatiana M. Kuplich and Ramon M. de Freitas, 2007. Mapping and monitoring land-cover in Corumbiara area, Brazilian Amazônia, using JERS-1 SAR multi-temporal data. In: *IEEE International Geoscience and Remote Sensing Symposium, 2007*, Barcelona, Spain, pp. 3370-3373.
- Tan, C.-P., J.-Y. Koay, K.-S. Lim, H.-T. Ewe and H.-T. Chuah, 2007. Classification of multi-temporal sar images for rice crops using combined entropy decomposition and support vector machine technique. *Progress In Electromagnetics Research*, PIER 71, 19-39.
- The World Watch Institute, 2007, *State of the World 2007: Our Urban Future* (W. W. Norton).
- Waske, B., Schiefer, S. and Braun, M., 2006. Random feature selection for decision tree classification of multi-temporal SAR data. In: *IEEE International Geoscience and Remote Sensing Symposium, 2006*, Denver, USA, pp.168-171.

ACKNOWLEDGEMENTS

The research was funded through a Swedish National Space Board grant. The RADARSAT-2 Fine-beam QuadPol SAR images were provided by the Canadian Space Agency through RADARSAT-2 Data for Research Use Program.